
Multi-Modal Prototypes for Open-Set Semantic Segmentation

Yuhuan Yang¹, Chaofan Ma¹, Chen Ju¹, Ya Zhang^{1,2}, Yanfeng Wang^{1,2}✉

¹ Coop. Medianet Innovation Center, Shanghai Jiao Tong University

² Shanghai AI Laboratory

{yangyuhuan, chaofanma, ju_chen, ya_zhang, wangyanfeng}@sjtu.edu.cn

Abstract

In semantic segmentation, adapting a visual system to novel object categories at inference time has always been both valuable and challenging. To enable such generalization, existing methods rely on either providing several support examples as visual cues or class names as textual cues. Through the development is relatively optimistic, these two lines have been studied in isolation, neglecting the complementary intrinsic of low-level visual and high-level language information. In this paper, we define a unified setting termed as open-set semantic segmentation (O3S), which aims to learn seen and unseen semantics from both visual examples and textual names. Our pipeline extracts multi-modal prototypes for segmentation task, by first single modal self-enhancement and aggregation, then multi-modal complementary fusion. To be specific, we aggregate visual features into several tokens as visual prototypes, and enhance the class name with detailed descriptions for textual prototype generation. The two modalities are then fused to generate multi-modal prototypes for final segmentation. On both PASCAL-5ⁱ and COCO-20ⁱ datasets, we conduct extensive experiments to evaluate the framework effectiveness. State-of-the-art results are achieved even on more detailed part-segmentation, Pascal-Animals, by only training on coarse-grained datasets. Thorough ablation studies are performed to dissect each component, both quantitatively and qualitatively.

1 Introduction

As one of the fundamental tasks in computer vision, semantic segmentation has made remarkable progress, with the development of large-scale datasets [27], and deep networks [41, 43, 7, 40]. Despite these advances, most studies [45, 51, 8] mainly focus on one closed-set scenario, where semantic categories remain identical for both training and inference. This assumption is an oversimplification of real-world deployment scenarios, hence limiting its practical uses.

In the recent literature, some studies consider one more challenging setting: training the vision system on seen categories, while handling both seen and unseen categories at inference time. To specify the unseen categories, there exist two lines, as shown in Fig. 1 (A). (1) Text-based [32, 26, 53, 24], *e.g.*, name or describe category in textual form. (2) Vision-based [47, 59, 49, 55], *e.g.*, give several image-mask examples as the support set. Although they have one shared goal, these two lines are still independent studies, and cannot enjoy the benefits of unity. More interesting, the lines of vision and text are complementary, making the lines unity profitable: (1) Low-level vision examples have rich contexts, which compensates for the textual informativeness in vanilla class names. (2) High-level text classes are semantically compact, which compensates for large visual variations in several examples.

Hence, this paper aims to jointly tackle these two lines with one unified model. And open-set semantic segmentation (O3S) is explicitly set to learn unseen semantics from both support visual examples and textual class names. This setting is practical as it frequently incorporates multi-modal human-model

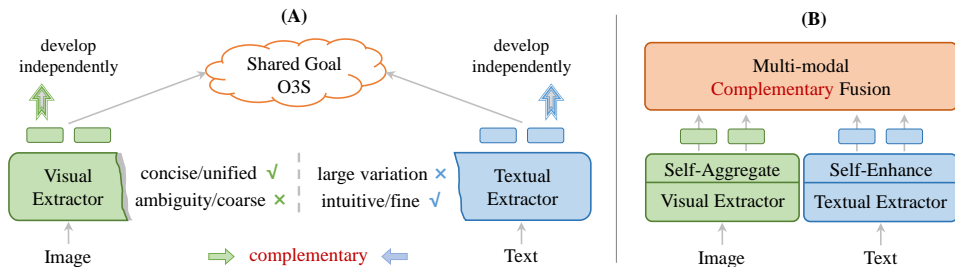


Figure 1: (A) Although having the shared goal, uni-modal prototypes are studied independently in existing literature, ignoring the complementarity between visual and textual data. (B) We unite the open-set task, and propose one novel multi-modal prototype extractor, with the design that first self-enhance and aggregate within the uni-modality, then fuse complementary knowledge between multi-modalities.

interaction in real world. Concretely, to better tackle O3S, we specially propose a novel multi-modal prototype extractor, with the design that first self-enhance and aggregate within the uni-modality, then fuse complementary knowledge between multi-modalities, as Fig. 1 (B) shows.

For the given textual class names, most existing works regard the embeddings of class names as textual prototypes. However, vanilla class names are always less informative in two ways: lexical ambiguity and lexical weak-tie. This is because the text representation is comprehensive and compressed intrinsically. The model may be confused when a single word can have multiple meanings. To avoid this, we enrich the context of single class name with multiple detailed descriptions in a self-enhanced way. The descriptions are automatically generated using large language models. For example, when talking about a cat, a chat robot can list several items as “four-legged body with a tail”, or “round eyes with vertically slit pupils”, which can accurately summarize the visual characteristics of a cat. These descriptions provide additional information that can eliminate ambiguity and enhance the discriminative power of the generated prototypes from the text encoder.

For the given visual support exemplars, they tend to be more intricate and plentiful, in contrast to text data. They can exhibit significant variations across regions, instances, and images, making it challenging to consolidate them into a unified representation. Here, we first aggregate foreground regions based on their coordinate, then apply masked average pooling on foreground features for each area. By adopting this approach, we are able to obtain a set of visual prototypes, with each prototype serving as an embedding center for a contiguous space.

To facilitate the cooperation between different modalities, we have incorporated a cross-attention mechanism for multi-modal fusion. This mechanism allows us to fuse the prototypes generated from different modalities, thereby enabling us to create a more comprehensive and accurate representation of the target object. And for final mask calculation, instead of widely-used single prototype projection, we are capable of handling multiple prototypes for a single class. Theoretically, multiple prototypes usually provide a more comprehensive and accurate representation than being aggregated into one. Thus, enabling multiple prototypes produces a more informative representation for each class, and making it promising for segmentation tasks.

On two datasets, namely, PASCAL-5ⁱ [9] and COCO-20ⁱ [27], our method achieves the new state-of-the-art. More exciting, our method also performs satisfactorily on a more detailed part-segmentation dataset, Pascal-Animals [34], without extra finetuning. Extensive ablations are conducted to dissect each component, both quantitatively and qualitatively. To sum up, our contributions lie in three folds:

- We unite an open-set setting for semantic segmentation (O3S), which jointly learns unseen category semantics from visual support samples and textual category names to facilitate the practicality.
- We design a multi-modal prototype framework for O3S, which first self-enhances and aggregates within intra-modality, then fuses complementarity from inter-modalities for better segmentation.
- We conduct extensive experiments and ablations to reveal complementarity between vision and text in O3S, and the superior performance of our multi-modal prototypes, on three standard datasets.

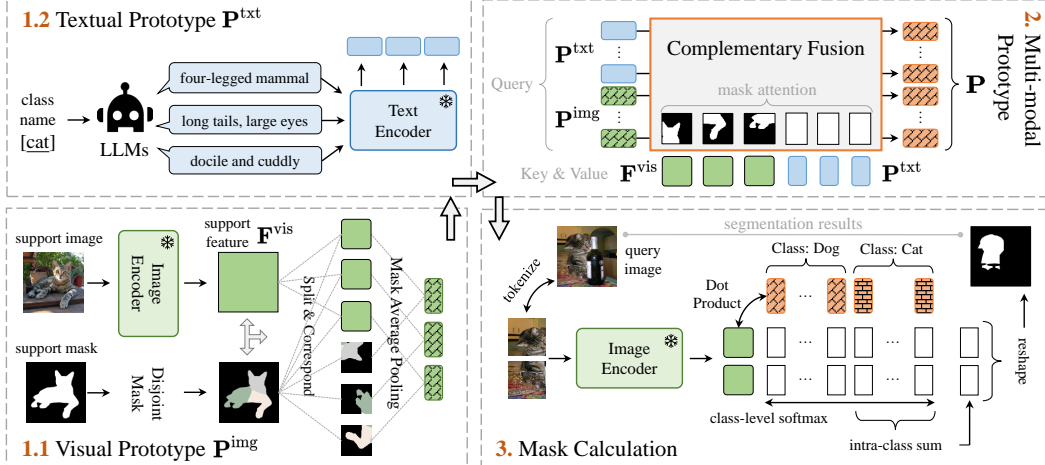


Figure 2: **Framework Overview.** (1.1) Visual prototypes through aggregation: we split support mask into parts and average visual feature on each part, forming several tokens as visual prototypes. (1.2) Textual prototypes through self-enhancement: to enrich the context and eliminate ambiguity, we use LLMs to generate informative and organized descriptions based on the given class name. (2) Fusing multi-modal prototypes: to advocate the complementary of visual and textual modality, we fuse prototypes from visual and textual modalities and get multi-modal prototypes. (3) Calculating mask: we consider multiple prototypes for one class as independent sub-class classifiers, and conduct intra-class sum as model output.

2 Related Work

Vision-Language Pre-training, also called “**foundation models**”, aims to align image-text embeddings training with large-scale web data. Recently, there have emerged many significant studies, *e.g.*, CLIP [39], ALIGN [16], Florence [56], FILIP [54], VideoCLIP [52], and LiT [57]. Structurally, these foundation pre-trainings usually contain one visual encoder and one textual encoder, which are trained using simple noise contrastive learning for powerful multi-modal representations. They have shown promising potential in many tasks: recognition [17, 21, 62], detection [31, 22, 18] and grounding [20, 19, 28]. In this paper, we use CLIP for open-vocabulary semantic segmentation, but the same technique should be applicable to other foundation models as well.

Few-shot Segmentation has gained significant attention in recent years due to its ability to classify novel classes with limited labeled samples. In terms of the utilization of support information, few-shot methods can be broadly divided into two categories: prototype based and dense feature based. Early works were mostly based on prototype learning [49, 47, 29], where one or multiple prototypes were generated from the support set samples and were used as a pixel-wise classifier [61] or fed into the decoder [58, 36, 30]. Another approach is to make full use of the dense support features [48, 60], by calculating pixel-to-pixel similarity based on 4D convolution [33] or attention-based methods [15]. However, these methods are mainly designed for binary setting, where only one novel class need to be segmented in each forward. Thus, another line of research focuses on improving the generality of few-shot methods. [46] extended the setting to let the model be able to predict all potential base and novel classes. And [13] proposed a simple baseline based on distilled information maximization loss. Different from above, we are the first to introduce text modality, and make contribution to architecture level exploration, while previous works mostly focused on training paradigm or loss functions.

Language-guided Open-vocabulary Segmentation (OVS) aims to understand novel categories in form of textual descriptions. Pioneering works either use generative models to synthesize visual features based on word embeddings [5, 25, 12] or employ a mapping process that assigns each pixel and semantic word to a joint embedding space [50, 2]. Recent researches have shown success on leveraging great power of pre-trained vision-language models (VLMs) for better image-text alignment [11, 24, 32]. Distinct from the above, we aim to understand novel categories in one more comprehensive way, with multi-modal involved.

3 Method

This paper aims to tackle open-set semantic segmentation, by multi-modal prototypes. We start by introducing task setup and motivation in Sec. 3.1; and then, we detail uni-modal prototype extraction for vision and text in Sec. 3.2, followed by multi-modal complementary fusion in Sec. 3.3; we detail mask calculation in Sec. 3.4; finally, we describe training and inference in Sec. 3.5.

3.1 Problem Formulation & Preliminary

Task Formulation. Given an image $\mathbf{I} \in \mathbb{R}^{H \times W \times 3}$ with height H and width W , open-set semantic segmentation (O3S) aims to train one model Φ to classify each pixel into \mathcal{C} semantic classes:

$$\mathbf{M} = \Phi(\mathbf{I}; \Theta) \in \{0, 1\}^{H \times W \times \mathcal{C}}. \quad (1)$$

Formally, during training, image-mask pairs from seen (base) classes $\mathcal{C}_{\text{seen}}$ are given, *i.e.*, $\{(\mathbf{I}, \mathbf{M}) \sim \mathcal{C}_{\text{seen}}\}$; while during testing, the model is evaluated beyond seen classes, *i.e.*, $\{\mathbf{I} \sim \mathcal{C}_{\text{seen}} \cup \mathcal{C}_{\text{unseen}}\}$.

Setting. To enable open-set capability, two ways have been explored to characterize novel semantics. One is open-vocabulary setting [32, 26, 53, 24], which provides **textual class names** for unseen classes *i.e.*, $\{\mathcal{T} \sim \mathcal{C}_{\text{unseen}}\}$. The other is few-shot setting [47, 59, 49, 55], which provides several image-mask (or image-bbox) **support exemplars** for unseen classes, *i.e.*, $\{\mathcal{S} = (\mathbf{I}, \mathbf{M}) \sim \mathcal{C}_{\text{unseen}}\}$. Since these two ways contains complementary knowledge with one shared goal, we here explicitly set O3S to learn unseen semantics from support visual examples and textual class names. Note that, such a setting is usually more practical in real-world scenarios.

Motivation. For O3S, the given support visual examples and textual class names are complementary, in terms of information. When texts are unsuitably long to capture all intricacies of category, “an image is worth a thousand words” to provide fine-grained details. When images exhibit large visual variability, “a word is worth a thousand images” to provide information-dense semantics for better generalization. To fully fuse such complementarity for O3S, this paper design a novel multi-modal prototype extractor, through intra-modal enhancement and multi-modal fusion. Specifically, **(1)** To address lexical ambiguity, we leverage the rich context of additional information that language affords, *i.e.*, sourcing visual descriptors of object categories from large language models. **(2)** To suppress intra-class variance, we propose to split the specific category of the image into different coarse regions, each with the same semantic meaning as fine-grained sub-categories. **(3)** To fuse visual and textual features, we propose a multi-modal complementary fusion mechanism that enables the model to focus on the most relevant information from both modalities.

Architecture Overview. As shown in Fig. 2, our proposed framework contains four main components, namely, one visual extractor Φ_{img} , one textual extractor Φ_{txt} , one multi-modal complementary fusion Φ_{fuse} and one mask calculator Φ_{mask} . For category semantics, Φ_{img} takes support exemplars $\mathcal{S} = \{(\mathbf{I}_s, \mathbf{M}_s)\}$ as inputs to output visual prototype \mathbf{P}^{img} ; while Φ_{txt} takes class names \mathcal{T} as inputs to output textual prototype \mathbf{P}^{txt} . And finally we use mask calculator Φ_{mask} to output mask using prototypes and query image \mathbf{I}_q . The above pipeline can be written as:

$$\hat{\mathbf{M}}_q = \Phi_{\text{mask}}(\mathbf{I}_q, \Phi_{\text{fuse}}(\mathbf{P}^{\text{img}}, \mathbf{P}^{\text{txt}})), \quad \mathbf{P}^{\text{img}} = \Phi_{\text{img}}(\mathbf{I}_s, \mathbf{M}_s), \quad \mathbf{P}^{\text{txt}} = \Phi_{\text{txt}}(\mathcal{T}). \quad (2)$$

3.2 Uni-modal Prototype Extractor: Visual Aggregation and Textual Enhancement

This subsection focuses on the extraction of prototypes for a single category. For both visual and textual modality, we extract several tokens as prototype separately.

3.2.1 Visual Extractor: Embedding Aggregation

With support images given, the large visual variations are key factors preventing them from forming accurate semantics. Hence, our goal is to aggregate semantics for variation mitigation.

Embeddings. For the given support set $\mathcal{S} = (\mathbf{I} \in \mathbb{R}^{H \times W \times 3}, \mathbf{M} \in \mathbb{R}^{H \times W \times \mathcal{C}})$, we adopt vision-language pre-training, namely, CLIP [39] for image embedding extraction. The resultant vision features are denoted as $\mathbf{F}^{\text{vis}} \in \mathbb{R}^{H \times W \times D}$, where D refers to the feature dimension.

Aggregation. To aggregate accurate semantics, a straightforward solution is masked-average-pooling Ψ_{map} , *i.e.*, masking the foreground area in images while ignoring the background parts, then

average-pooling foreground features from \mathbf{F}^{vis} as the prototype embeddings \mathbf{p} . Formally,

$$\mathbf{p} = \Psi_{\text{map}}(\mathbf{F}^{\text{vis}}, \mathbf{M}) = \left(\sum_{i=1}^H \sum_{j=1}^W \mathbf{F}_{i,j}^{\text{vis}} \cdot \mathbf{M}_{i,j} \right) / \left(\sum_{i=1}^H \sum_{j=1}^W \mathbf{M}_{i,j} \right) \in \mathbb{R}^D. \quad (3)$$

However, Ψ_{map} may be insufficient for segmentation, since over-general pooling can ignore the visual variance between regions and instances. To finely exploit visual information from the support set, some few-shot methods [48, 60] turn to directly calculate pixel-wise similarity for each class of interest, but this leads to high consuming of time and computation. To address the over-general issue while maintain low consuming, we introduce a multiple-masked-average pooling $\Psi_{\text{m-map}}$. Specifically, we first split mask \mathbf{M} into n non-overlapping areas: $\{\mathbf{M}_1, \mathbf{M}_2, \dots, \mathbf{M}_n\}$; and then calculate visual embeddings through masked-average-pooling Ψ_{map} for each area; finally, we concatenate all area embeddings to form the prototype for the whole image:

$$\mathbf{P}^{\text{img}} = \Psi_{\text{m-map}}(\mathbf{F}^{\text{vis}}, \mathbf{M}) = [\Psi_{\text{map}}(\mathbf{F}^{\text{vis}}, \mathbf{M}_1), \dots, \Psi_{\text{map}}(\mathbf{F}^{\text{vis}}, \mathbf{M}_n)] \in \mathbb{R}^{n \times D}, \quad (4)$$

where $[\cdot, \dots, \cdot]$ means embedding concatenation. To split \mathbf{M} into non-overlapping areas, we use a Voronoi-based method [1] to save computational costs, since it only considers coordinate distance with no need for gradient back-propagation. See appendix for more implementation details.

3.2.2 Textual Extractor: Class Name Enhancement

For the given names of unseen classes, information ambiguity is a key factor preventing them from forming clear semantics. Hence, our goal is to enhance them by descriptions for disambiguation.

Vanilla Class Names are directly used to calculate text semantic prototypes in some recent studies [24, 32]. However, such an idea usually results in prototypes with ambiguous discrimination, because class names are compact with limited or biased information. (1) **Lexical ambiguity**. Class name usually consists of one or two words, *e.g.*, “crane” can refer to either a bird or a machine. (2) **Lexical weak-tie**. Sometimes the connection between class name and its literal meaning is weak. For instance, there is little visual similarity between Pomeranian dog and Pomerania location. Rather, Pomeranian dogs are typically differentiated based on their fox-like faces, fluffy fur, and small size.

Informative Descriptions. To solve the above issues, enriching vanilla class names with detailed descriptions is promising to bring more comprehensive semantic knowledge, *e.g.* replacing “Pomeranian dogs” with “Pomeranian dog is a species of dog with fox-like faces.” will increase the discriminating power of prototype generated by text encoder. However, such hand-crafted summarizations are largely products of human observation and experience, thus been both time-consuming and difficult to scale up, limiting the real-world applications.

Here, we turn our sights to large-scale language models (LLMs) [4, 38], which are pre-trained on large corpora of data, for their remarkable performance of semantic understanding and text generation. To automatically adapt LLMs Ψ_{llm} to enrich class contexts, we propose a robust querying instruction that helps to generate well-organized answers while filtering out irrelevant descriptions.

Intuitively, we want to let the LLM list as much information as possible. Besides, to establish an automatic parsing pipeline, the answer of LLM should match a specific pattern. We first try to ask them directly as: “What does a Pomeranian dog looks like? List by items.” This will result in one organized answer like:

- Size: Pomeranians are small dogs, typically weighing between 3-7 pounds ...
- Coat: Pomeranians have a thick, fluffy double coat of fur that comes in a variety of colors.
- Behavior: Pomeranians are known for their energetic and playful nature ...

By parsing the answer using \bullet as indicator, we can get a list of descriptions for Pomeranian dogs, each describe the current species from a different view. However, the above description contains some abstract concepts which can not be directly seen in an image, such as the “energetic and playful” in “Behavior” item. Thus, instead of simply asking “what does it looks like”, we need to add some constraints on the question. For example, we may ask: “What are some visual features for distinguishing Pomeranian dogs in an image?” By highlighting “visual features” and “in an image” we are able to filter out those abstract concepts. We can also provide handwritten examples before asking questions to lead the answer into wanted format. For more

discussion about prompt we refer to our supplementary material. After parsing the answer given, we are able to form a list of detailed descriptions for class of interest. Taking class name \mathcal{T} for an example, the above process can be formulated as:

$$\mathcal{T}^{\text{txt}} = \{\mathcal{T}_1^{\text{txt}}, \mathcal{T}_2^{\text{txt}}, \dots, \mathcal{T}_n^{\text{txt}}\} = \Psi_{\text{llm}}(\mathcal{T}), \quad (5)$$

where $\mathcal{T}_1^{\text{txt}}, \mathcal{T}_2^{\text{txt}}, \dots, \mathcal{T}_n^{\text{txt}}$ are n descriptions depicting the current class from different perspective. Note that the number of descriptions is flexible to select, and here for simplicity, we use the same number as the visual side.

Embeddings. By asking LLMs and parsing the answers, we can get a list of context descriptions \mathcal{T}^{txt} for each class. Then, we combine \mathcal{T}^{txt} with vanilla class names, feed into CLIP [39] for text-modal embeddings. The resultant embeddings are our text-modal prototypes, denoted as $\mathbf{P}^{\text{txt}} \in \mathbb{R}^{n \times D}$.

3.3 Multi-Modal Fusion: Knowledge Alignment & Complementarity

As discussed in Sec. 1, visual and textual prototypes are complementary. To advocate such complementarity, we here interact prototypes from these two modalities for knowledge alignment and comprehensive fusion, further forming our multi-modal prototypes.

Attention-based Fusion. Here we employ the cross-attention mechanism to achieve our goal. Specifically, we treat the two modality equally, and the query for attention is the matrix concation of multi-modal prototypes: $\mathbf{Q} = [\mathbf{P}^{\text{txt}}, \mathbf{P}^{\text{img}}] \in \mathbb{R}^{2n \times D}$. n prototypes for each modality separately. We aim to integrate both visual and textual information as references in order to generate more comprehensive multi-modal prototypes. Notice that \mathbf{P}^{img} contains only foreground information, but we consider some background information also to be helpful. Therefore, we select \mathbf{K} and \mathbf{V} by concatenating \mathbf{P}^{txt} with the dense image feature: $\mathbf{K}, \mathbf{V} = [\mathbf{P}^{\text{txt}}, \mathbf{F}^{\text{vis}}]$. \mathbf{F}^{vis} is the result by forwarding image into visual encoder.

Foreground-Background Balance. To balance the importance of foreground and background, we introduce a learnable weighted mask on the background portion of attention score, thus weakening the effect of background on output results. This allows the model to absorb background information during training without being overwhelmed by it. The multi-modal prototypes are fused through:

$$\mathbf{P} = \Phi_{\text{fuse}}(\mathbf{P}^{\text{txt}}, \mathbf{P}^{\text{img}}) = \sigma\left(\frac{\mathbf{K}^T \mathbf{Q}}{\sqrt{D}} - \alpha \cdot \overline{\mathbf{M}}\right) \cdot \mathbf{V} \in \mathbb{R}^{2n \times D}. \quad (6)$$

Here $\overline{\mathbf{M}}$ gets non-zero only on features representing background patches. α is a learnable parameter for foreground-background balance. When $\alpha \rightarrow \infty$, the output is only relevant with foreground features, no background features are involved. σ is the softmax function.

3.4 Mask Calculation with Multiple Prototypes

We denote $\mathbf{P}_i \in \mathbb{R}^{2n \times D}$ as prototypes for class i , which can be seen as $2n$ different prototypes describing the class of interest from different perspectives. By concatenating prototypes \mathbf{P}_i through all classes, we get $\tilde{\mathbf{P}} \in \mathbb{R}^{2n|\mathcal{C}| \times D}$, which means there's $2n|\mathcal{C}|$ different prototypes in total.

$$\tilde{\mathbf{P}} = [\mathbf{P}_1, \mathbf{P}_2, \dots, \mathbf{P}_{|\mathcal{C}|}] \in \mathbb{R}^{2n|\mathcal{C}| \times D}. \quad (7)$$

$\tilde{\mathbf{P}}$ can be divided into $|\mathcal{C}|$ semantic groups, each containing $2n$ prototypes describing one class. The query image is passed through visual encoder to get query feature $\mathbf{F}_q \in \mathbb{R}^{HW \times D}$. After that, we calculate the class-wise probability by first seeing each prototype as an independent classifier, and then aggregating the total $2n$ probabilities within a semantic group using Φ_{agg} . Formally:

$$\hat{\mathbf{M}}_q = \Phi_{\text{agg}}\left(\sigma(\mathbf{F}_q \cdot \tilde{\mathbf{P}}^T)\right) \in \mathbb{R}^{HW \times |\mathcal{C}|}, \quad (8)$$

where $\hat{\mathbf{M}}_q$ is the model output and σ refers to the softmax. Φ_{agg} is a naive summation in practice.

Discussion. Theoretically, multiple number of vectors usually contains more information than a single one, even if the latter is the aggregation of the formers. Most open-vocabulary methods use a one-dimensional vector as the final prototype, aiming to aggregate all semantic information into a single vector. This design indeed compresses information, but also brings informational bottleneck,

especially when the semantic concept is sophisticated to describe. By enabling the existence of multiple prototypes for one class, we are able to express more comprehensive information, and describe the current class from different perspectives.

Multi-Level Fusion. In practice, as objects usually vary in scale, multi-level visual modeling is crucial, given that the last-layer output from the visual encoder sometimes loose detailed information. Specifically, we consider totally L intermediate layers to form multi-level feature pyramid. For each level we are able to give out a coarse mask prediction, forming: $\{\hat{\mathbf{M}}_q^l\}_{l=1}^L$. We fuse results of multi level together and get the final prediction $\hat{\mathbf{M}}_q^{\text{final}}$. Note that for the purpose of generalization, the whole fusion strategy is designed to be class-agnostic.

3.5 Training and Inference

During training, O3S provides pixel-wise annotations $\mathbf{M}_q \in \{0, 1\}^{HW \times |\mathcal{C}_{\text{seen}}|}$ on seen classes $\mathcal{C}_{\text{seen}}$ for supervision. To optimize our multi-modal prototype framework, we use the cross-entropy loss \mathcal{L}_{CE} over final mask $\hat{\mathbf{M}}_q^{\text{final}}$ as well as those intermediate masks $\hat{\mathbf{M}}_q^l$ before fusion:

$$\mathcal{L}_{\text{all}} = \mathcal{L}_{\text{CE}}(\hat{\mathbf{M}}_q^{\text{final}}, \mathbf{M}_q) + \lambda \sum_{l=1}^L \mathcal{L}_{\text{CE}}(\hat{\mathbf{M}}_q^l, \mathbf{M}_q), \quad (9)$$

where λ is a balancing ratio. Note that, throughout training, CLIP encoders and LLMs are frozen for two reasons: (1) Reducing computational burden. (2) Frozen models preserve the prior knowledge of multi-modal alignment, and also ensure good generalization to avoid overfitting seen classes.

At inference time, we first calculate multi-modal prototypes for unseen classes using visual support examples and textual class names, then concatenate them together with multi-modal prototypes from seen classes for segmentation, the other pipeline remains the same as training.

4 Experiments

4.1 Comparison with State-of-the-Art

Dataset. Here we evaluate on two widely-used benchmarks. PASCAL-5ⁱ [9, 14, 42] has 20 classes in total. Classes are evenly split into four folds, each fold containing 5 classes. The model is trained with classes from three folds as seen and the rest as unseen. Unseen classes are marked as ignored during training. For inference, both seen and unseen classes should be segmented out. COCO-20ⁱ [27, 42] is composed of 80 classes, with 20 classes each fold in a similar vein. Following [13], we use all available query images for PASCAL-5ⁱ and sample 10k images for COCO-20ⁱ.

Evaluation Metrics. We report mIoU of each fold as well as average across 4 folds. **Seen** means mIoU over $\mathcal{C}_{\text{seen}}$ and **UnSeen** is the mIoU over $\mathcal{C}_{\text{unseen}}$. Following [55] we also report the harmonic mean **HIoU** of **Seen** and **UnSeen** to show model’s generalized segmentation.

Implementation details. For fair comparison, all experiments are conducted on CLIP ResNet50 backbone. As ResNet encoder uses progressive downsampling, we extract all inner features smaller than 1/4 resolution. Features with same resolution shares the same model parameter. We set the number of prototypes for single modality $n = 3$, and loss weight $\lambda = 0.01$. We treat background as a special class in $\mathcal{C}_{\text{seen}}$. SGD optimizer is used with learning rate $lr = 1e - 3$. For LLMs, we use OpenAI api on calling `gpt-4` [38] model. All experiments are conducted using 2 NVIDIA RTX A6000 GPUs.

Results. Tab. 1 shows the results. Our method outperforms state-of-the-art DIaM by 4.33% on **UnSeen** metric under 1-shot setting on PASCAL-5ⁱ. This indicates that introducing text as guidance helps generalizing to novel categories. Besides, our method also achieves the best **HIoU** score, which means our model can segment both seen and unseen classes well at the same time.

4.2 Fine-Grained Transfer

Here to present the model’s transferability towards fine-grained dataset, we use checkpoints from Sec. 4.1 and directly applied them to the part-segmentation dataset. Checkpoints trained on fold-0 of PASCAL-5ⁱ are used for testing.

Table 1: **Comparison with SOTA methods on PASCAL-5ⁱ and COCO-20ⁱ.** We report mean results over all 5 folds. **HIoU** is the harmonic mean of **Seen** and **UnSeen**. Our method achieves the best **HIoU** on both datasets, and a significant improvement on **UnSeen** categories, indicating the strong generalization to novel categories.

Method	Year	PASCAL-5 ⁱ						COCO-20 ⁱ		
		Seen	1-Shot UnSeen	HIoU	Seen	5-Shot UnSeen	HIoU	Seen	1-Shot UnSeen	HIoU
CANet [59]	CVPR'19	8.73	2.42	3.79	9.05	1.52	5.29	-	-	-
PANet [49]	ICCV'19	31.88	11.25	16.63	32.95	15.25	24.1	-	-	-
PFENet [47]	TPAMI'20	8.32	2.67	4.04	8.83	1.89	5.36	-	-	-
MiB [6]	CVPR'20	63.80	8.86	15.56	68.60	28.93	48.77	-	-	-
SCL [58]	CVPR'21	8.88	2.44	3.38	9.11	1.83	5.47	-	-	-
RePRI [3]	CVPR'21	20.76	10.50	13.95	34.06	20.98	27.52	5.62	4.74	5.14
CAPL [46]	CVPR'22	64.80	17.46	27.51	65.43	24.43	44.93	43.21	7.21	12.36
BAM [23]	CVPR'22	71.60	27.49	39.73	71.60	28.96	50.28	49.84	14.16	22.05
DlaM [13]	CVPR'23	70.89	35.11	46.96	70.85	55.31	63.08	48.28	17.22	25.39
Ours	-	71.20	39.44	50.76	72.22	57.53	64.04	45.83	19.48	27.34

Dataset & Metric. We use Pascal-Animals, a part-segmentation dataset with pixel-wise labels. Following [34], we consider five quadruped animals in this dataset: *Cat*, *Cow*, *Dog*, *Horse* and *Sheep*. For each animal we apply the same filter as [34] did and get totally 2872 images from the five classes (893 *Cat*, 233 *Cow*, 1097 *Dog*, 404 *Horse*, 245 *Sheep*). We consider four parts for each animal: *head*, *torso*, *legs* and *tail*. We report the mIoU over four parts as our evaluation metric.

Baselines. Here we compare with other few-shot methods under 1-shot setting, which means one image-mask pair is given for each part of the four segmentation area. For both our model and other baselines, we take checkpoints trained under fold-0 of PASCAL-5ⁱ for fair comparison. We also take the results from [10, 35, 37, 44] as in-domain upper bounds. In in-domain setting, models are trained using annotations from four animals and tested on the rest one.

Results. Tab. 2 shows the performance of our method and other baselines. The results show that the proposed method outperforms other few-shot methods on all animal categories, achieving the highest mIoU scores, and is even comparable with some in-domain methods.

Table 2: **Fine-grained Part-Segmentation.** “Transfer” means using pre-trained checkpoints with only one-shot example provided, no extra finetuning. “In-domain” means the model is trained on four animals with fine-grained annotation and tested on the remaining one. Our method achieves best among all transfer settings, and is even comparable with several in-domain methods.

Method	Setting	Cat	Cow	Dog	Horse	Sheep
DlaM [13]	Transfer	28.59	24.48	25.79	24.76	24.89
Ours	Transfer	34.72	33.76	34.46	34.08	34.84
RefineNet [10]	In-domain	11.87	12.96	11.72	11.84	13.16
Transform [35]	In-domain	33.06	38.90	37.42	37.31	39.25
Hourglass [37]	In-domain	32.56	43.73	35.34	40.59	46.37
TernausNet [44]	In-domain	42.65	48.37	44.03	50.92	50.90

4.3 Ablation Studies

Here, we thoroughly examine how the model’s performance is influenced by the provision and processing of both textual and visual information. First, we investigate on the situation where provided information is incomplete, weakened, or missing in either the visual or textual modality. We systematically weaken the information provided in each modality to analyze the model’s ability to handle such scenarios (Tab. 3). Additionally, we also investigate the impact of prototype extraction, which involves controlling the granularity of image partitioning through image prototype number, and controlling the level of detail in class descriptions through text prototype number (Tab. 4). All ablation studies are done on fold-2 of PASCAL-5ⁱ under 1-shot setting. This fold has the lowest **UnSeen** mIoU, indicating most hard for base-to-novel adaptation.

Table 3: **Ablation study on provided information.** ①-③ for textual information, ④-⑤ ablate the visual part. Both visual and textual information contributes to the final result.

	Visual		Textual		Seen	UnSeen	HIoU
	Img	Anno	Name	Desc			
①	✓	mask	✓	✓	69.81	32.31	44.17
②	✓	mask	✓	-	68.91	30.59	42.37
③	✓	mask	-	-	69.10	27.09	38.92
④	✓	box	✓	✓	62.39	24.32	35.00
⑤	-	-	✓	✓	61.58	21.50	31.87

Table 4: **Ablation on the prototype processing.** N-VPT / N-TPT are short for “Number of Visual / Textual Prototype”. **Left:** More visual prototypes shows steady improvement. **Right:** Increasing textual prototype number helps better describe classes and brings performance. However, over large number may introduce noise.

N-VPT	Seen	UnSeen	HIoU	N-TPT	Seen	UnSeen	HIoU
1	68.82	27.59	39.39	1	69.21	30.53	42.37
3	69.81	32.31	44.17	3	69.81	32.31	44.17
5	70.21	33.53	45.39	5	70.32	29.85	41.91



Figure 3: **Visualization of 5-Shot Results From PASCAL-5^t.** With bus, car, cat, chair, cow as unseen classes. Our model can segment both seen and unseen classes well.

Different Information Provided. Our method requires detailed description about class names as well as pixel-wise mask annotations for each class as support. Here we investigate on the situation where the information is incomplete, weakened, or missing. For textual side, we remove class description (②). For visual side, we weaken the support information, by replacing mask annotations with bounding-boxes (④). We have also tested on single-modal situation (③, ⑤).

Tab. 3 shows the ablation results. There’s no doubt that experiment ① with full support information achieves the highest performance. Comparing ② and ③ with ① we find that enriching textual context with detailed information could largely improve the performance. Besides, pixel-wise annotation for support image is also important, since it provides an accurate indication of whether a foreground should look like. Loosing this constrains to box annotations will surely introduce noise into vision prototype representation (④). Last, our model showed acceptable performance even when all image information was absent (⑤), suggesting that our model is robust in extreme scenarios.

Prototype Processing. The number of prototypes used for visual and textual modality is a key hyperparameter through the whole pipeline. Image prototype number determines the granularity of image partitioning, while text prototype number shows how detailed the class description is. Here we vary the prototype number of one modality while keeping the other one fixed.

Tab. 4 shows the ablation results. For visual modality, larger number of prototypes shows steady improvement. This is because compared with hundreds number of foreground pixels, the prototype number is relatively small. Increasing the number of prototypes in the textual modality can improve the performance by providing more detailed descriptions. However, if the number beyond a certain point, the performance drops. This is because typical visual features may not appear concurrently within a single image, thus listing too many descriptions at once may introduce noise.

4.4 Visualization

Fig. 3 shows some visualization results from PASCAL-5^t under 5-shot setting. The classes bus, car, cat, chair, cow are treated as unseen. We can see that our model can segment both seen and unseen well at the same time.

5 Conclusion

To conclude, this paper introduces a novel approach to open-set semantic segmentation (O3S) that enables the learning of unseen semantics from both textual and visual modalities. The proposed framework extracts prototypes from each modality separately and fuses them to generate multi-modal

prototypes for final segmentation. By enriching the textual class names with detailed descriptions and aggregating visual features, the proposed method achieves state-of-the-art results on both PASCAL-5ⁱ and COCO-20ⁱ datasets and performs satisfactorily on the more detailed Pascal-Animals part-segmentation with one-shot transfer. We hope this work can motivate researchers to utilize multi-modal information for more effective and comprehensive algorithm design in the future.

Limitations and Future Works. Currently, our model select textual descriptions from candidate list in a fully random manner, which may not fit the content of image perfectly. In future work we will focus on the selection policy for most suitable textual descriptions.

A Appendix

A.1 Pipeline details

Here we supplement some details about model building, which could not be mentioned in the main paper due to space limitations. We detail how we separate masks into parts in Sec. A.1.1, and provide different versions of prompts for asking large language models (LLMs) in Sec. A.1.2. We also show how to extend our method to K-shots setting in Sec. A.1.3.

A.1.1 Voronoi-Based Partition Algorithm

We use a Voronoi-based algorithm [1] to split mask into different partitions. This algorithm only considers coordinate distance with no need for gradient back-propagation. The algorithm randomly selects initial semantic center, and choose the farthest pixel from known ones as the new center iteratively. The algorithm is shown in Alg. 1.

Fig. 4 shows two examples of gradually increasing partition number. The algorithm is able to separate different instances and different area within the same instance.

Algorithm 1: Partition Algorithm

Input : Binary mask \mathbf{M} , number to partition n .

Output : A partition of the map $\{\mathbf{M}_1, \mathbf{M}_2, \dots, \mathbf{M}_n\}$

```

1  $\mathcal{U} \leftarrow \{t = (i, j) | \mathbf{M}[i, j] = 1\};$  // Union set: all foreground pixels
2 random select  $t_1 \in \mathcal{U};$ 
3  $\mathcal{P} = \{t_1\};$  // First seed init randomly
4 for  $i \leftarrow 2$  to  $n$  do
5    $t_i = \arg \max_{t \in \mathcal{U}} \min_{t_j \in \mathcal{P}} \|t - t_j\|_2;$ 
6    $\mathcal{P} \leftarrow \mathcal{P} \cup \{t_i\};$  // Add new seed
7 foreach  $\mathbf{M}_k, k \in \{1, 2, \dots, n\}$  do init  $\mathbf{M}_k$  as all zero;
8 for  $t = (i, j) \in \mathcal{U}$  do
9    $k = \arg \min_{\{1, 2, \dots, n\}} \|t - t_k\|_2;$ 
10   $\mathbf{M}_k[i, j] = 1;$  // Assign to the nearest seed
```

A.1.2 Prompting LLMs

Here we list more prompts for asking GPT-4 and their responses.

Direct prompts. First we ask the GPT-4 in the most direct way as:

What does Pomeranian dogs look like? List by items.

This will result in the following response:

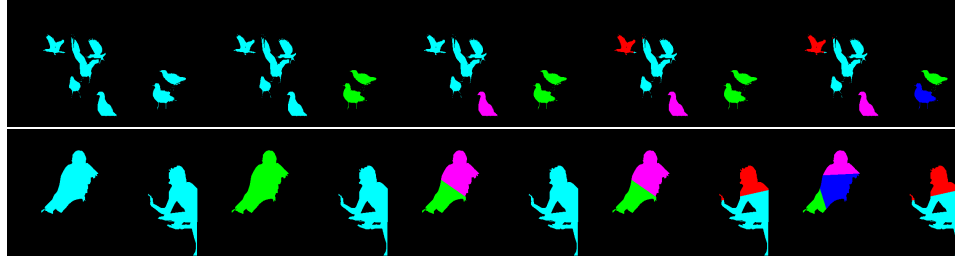


Figure 4: **Examples for partition algorithm.** While increasing the partition number from 1 to 5, the algorithm is able to separate different instances and different area within the same instance.

Sure, here are some characteristics of Pomeranian dogs:

- **Size:** Pomeranians are a small breed, typically weighing between 3 and 7 pounds and standing about 6 to 7 inches tall at the shoulder.
- **Coat:** Pomeranians have a thick, double coat that comes in a variety of colors including black, brown, orange, cream, white, blue, and sable. The outer coat is long and straight, while the undercoat is soft and dense.
- **Face:** Pomeranians have a fox-like face with small, pointed ears and a short, compact muzzle. They have dark, almond-shaped eyes and a black nose.
- **Body:** Pomeranians have a compact, sturdy body with a level topline and a curled tail that rests on their back.
- **Personality:** Pomeranians are known for their lively, friendly, and energetic personalities. They are intelligent, curious, and eager to please, but can also be stubborn and independent at times.

However, the above result is not satisfactorily in two aspects: (1) It contains some abstract descriptions that can not be directly seen in a photo, such as “personality”. (2) Some descriptions are too long to be dealt with. To avoid this, we need to add some constrains on the questions we ask.

Constrained prompts. The modified version of prompt takes more control about the sentence length and content of the generated results:

What are some visual features for distinguishing Pomeranian dogs in a photo? List by items, with no more than 30 words each item.

And the result is:

- **Size:** Pomeranians are typically small dogs, weighing between 3 and 7 pounds.
- **Coat:** Their double coat is fluffy and thick, commonly in shades of orange, red, cream, black, or sable.
- **Face:** Pomeranians have a distinctive foxy face with a short muzzle and upright ears.
- **Tail:** Their tail is plumed and curls over their back.
- **Proportions:** Pomeranians have a compact body with a short back, giving them a distinct "cobby" appearance.
- **Eyes:** Their eyes are round and dark, often with an alert and intelligent expression.
- **Movement:** Pomeranians have a bouncy, almost prancing gait.
- **Features:** Other distinguishing features include a small, black nose and small, round feet.

Prompts with examples. Another way to force the GPT-4 to generate descriptions in exactly the format we want is to provide some examples. We take the above answer for Pomeranians dogs as an example, and ask the GPT-4 to generate descriptions for other classes in the same format:

For each object I give, list more than 10 most useful visual features about this object in the following format, with each item no more than 30 words. For example:
Pomeranian dog?

- Size: Pomeranians are small dogs, typically weighing between 3-7 pounds
 - Coat: Pomeranians have a thick, fluffy double coat of fur that comes in a variety of colors
- Now please answer.

Here we provide some example responses for classes in PASCAL-5ⁱ dataset.

Class name: **cat**

- Size: Cats come in various sizes, but most domestic cats are small to medium-sized, usually weighing between 5-15 pounds.
- Body shape: Cats have a slender and agile body with flexible bones that allow them to move in various ways.
- Coat: Cats have a fur coat that can be short, long, or medium in length, and it can come in various colors and patterns.
- Eyes: Cats have large, round eyes that can come in different colors, such as green, yellow, blue, or brown.
- Ears: Cats have pointed ears that are usually upright and have a range of motion to help them detect sounds and communicate.
- Whiskers: Cats have long and sensitive whiskers on their cheeks, chin, and above their eyes that help them gauge distances and navigate in the dark.
- Teeth: Cats have sharp teeth that are adapted for hunting and eating meat.
- Claws: Cats have retractable claws that they can extend or retract to help them climb, scratch, or defend themselves.
- Tail: Cats have a long and flexible tail that helps them maintain balance and communicate their mood.
- Paws: Cats have soft and padded paws with five toes on their front feet and four toes on their back feet that help them walk, run, and climb.

Class name: **aeroplane**

- Fuselage: The fuselage is the main body of the airplane that holds the cockpit and passengers or cargo.
- Wings: The wings are the flat surfaces on either side of the fuselage that generate lift and allow the airplane to fly.
- Engines: Airplanes can have one or more engines mounted on the wings or fuselage that provide thrust for propulsion.
- Tail: The tail is located at the rear of the airplane and consists of the vertical stabilizer, horizontal stabilizer, and rudder.
- Cockpit: The cockpit is the area where the pilots sit and control the airplane.
- Windows: Airplanes have multiple windows on the sides of the fuselage that allow passengers to see outside during flight.
- Landing gear: Airplanes have retractable landing gear that allows them to take off and land on runways.
- Nose: The nose of the airplane is the front section of the fuselage and can have a variety of shapes depending on the type of airplane.
- Winglets: Some airplanes have winglets on the tips of the wings that reduce drag and increase fuel efficiency.
- Paint scheme: Airplanes can have unique paint schemes and designs that help identify the airline or organization that operates them.
- Antennas: Airplanes can have various antennas on the fuselage and wings for communication and navigation purposes.

References

- [1] Franz Aurenhammer. Voronoi diagrams—a survey of a fundamental geometric data structure. *ACM Computing Surveys (CSUR)*, 1991.
- [2] Donghyeon Baek, Youngmin Oh, and Bumsub Ham. Exploiting a joint embedding space for generalized zero-shot semantic segmentation. In *Proceedings of the International Conference on Computer Vision*, 2021.
- [3] Malik Boudiaf, Hoel Kervadec, Ziko Imtiaz Masud, Pablo Piantanida, Ismail Ben Ayed, and Jose Dolz. Few-shot segmentation without meta-learning: A good transductive inference is all you need? In *Proceedings of the IEEE Conference on Computer Vision and Pattern Recognition*, 2021.
- [4] Tom Brown, Benjamin Mann, Nick Ryder, Melanie Subbiah, Jared D Kaplan, Prafulla Dhariwal, Arvind Neelakantan, Pranav Shyam, Girish Sastry, Amanda Askell, et al. Language models are few-shot learners. *Advances in Neural Information Processing Systems*, 2020.
- [5] Maxime Bucher, Tuan-Hung Vu, Matthieu Cord, and Patrick Pérez. Zero-shot semantic segmentation. *Advances in Neural Information Processing Systems*, 2019.
- [6] Fabio Cermelli, Massimiliano Mancini, Samuel Rota Buló, Elisa Ricci, and Barbara Caputo. Modeling the background for incremental learning in semantic segmentation. *Proceedings of the IEEE Conference on Computer Vision and Pattern Recognition*, 2020.
- [7] Liang-Chieh Chen, George Papandreou, Iasonas Kokkinos, Kevin Murphy, and Alan L Yuille. Deeplab: Semantic image segmentation with deep convolutional nets, atrous convolution, and fully connected crfs. *IEEE Transactions on Pattern Analysis and Machine Intelligence*, 2017.
- [8] Bowen Cheng, Alexander G. Schwing, and Alexander Kirillov. Per-pixel classification is not all you need for semantic segmentation. In *Advances in Neural Information Processing Systems*, 2021.
- [9] Mark Everingham, SM Eslami, Luc Van Gool, Christopher KI Williams, John Winn, and Andrew Zisserman. The pascal visual object classes challenge: A retrospective. *International Journal of Computer Vision*, 2015.
- [10] Hao-Shu Fang, Guansong Lu, Xiaolin Fang, Jianwen Xie, Yu-Wing Tai, and Cewu Lu. Weakly and semi supervised human body part parsing via pose-guided knowledge transfer. *Proceedings of the IEEE Conference on Computer Vision and Pattern Recognition*, 2018.
- [11] Golnaz Ghiasi, Xiuye Gu, Yin Cui, and Tsung-Yi Lin. Scaling open-vocabulary image segmentation with image-level labels. In *Proceedings of the European Conference on Computer Vision*, 2022.
- [12] Zhangxuan Gu, Siyuan Zhou, Li Niu, Zihan Zhao, and Liqing Zhang. Context-aware feature generation for zero-shot semantic segmentation. In *Proceedings of the 28th ACM International Conference on Multimedia*, 2020.
- [13] Sina Hajimiri, Malik Boudiaf, Ismail Ben Ayed, and Jose Dolz. A strong baseline for generalized few-shot semantic segmentation. In *Proceedings of the IEEE Conference on Computer Vision and Pattern Recognition*, 2023.
- [14] Bharath Hariharan, Pablo Arbeláez, Ross Girshick, and Jitendra Malik. Simultaneous detection and segmentation. In *Proceedings of the European Conference on Computer Vision*, 2014.
- [15] Sunghwan Hong, Seokju Cho, Jisu Nam, and Seungryong Kim. Cost aggregation is all you need for few-shot segmentation. *arXiv:2112.11685 [cs]*, 2021.
- [16] Chao Jia, Yinfei Yang, Ye Xia, Yi-Ting Chen, Zarana Parekh, Hieu Pham, Quoc V. Le, Yunhsuan Sung, Zhen Li, and Tom Duerig. Scaling up visual and vision-language representation learning with noisy text supervision. In *Proceedings of the International Conference on Machine Learning*, 2021.
- [17] Chen Ju, Tengda Han, Kunhao Zheng, Ya Zhang, and Weidi Xie. Prompting visual-language models for efficient video understanding. In *Proceedings of the European Conference on Computer Vision*, 2022.
- [18] Chen Ju, Zeqian Li, Peisen Zhao, Ya Zhang, Xiaopeng Zhang, Qi Tian, Yanfeng Wang, and Weidi Xie. Multi-modal prompting for low-shot temporal action localization. *arXiv preprint arXiv:2303.11732*, 2023.
- [19] Chen Ju, Haicheng Wang, Jinxiang Liu, Chaofan Ma, Ya Zhang, Peisen Zhao, Jianlong Chang, and Qi Tian. Constraint and union for partially-supervised temporal sentence grounding. *arXiv preprint arXiv:2302.09850*, 2023.

- [20] Chen Ju, Peisen Zhao, Siheng Chen, Ya Zhang, Yanfeng Wang, and Qi Tian. Divide and conquer for single-frame temporal action localization. In *Proceedings of the International Conference on Computer Vision*, 2021.
- [21] Chen Ju, Peisen Zhao, Siheng Chen, Ya Zhang, Xiaoyun Zhang, Yanfeng Wang, and Qi Tian. Adaptive mutual supervision for weakly-supervised temporal action localization. *IEEE Transactions on Multimedia*, 2022.
- [22] Chen Ju, Kunhao Zheng, Jinxiang Liu, Peisen Zhao, Ya Zhang, Jianlong Chang, Qi Tian, and Yanfeng Wang. Distilling vision-language pre-training to collaborate with weakly-supervised temporal action localization. In *Proceedings of the IEEE Conference on Computer Vision and Pattern Recognition*, 2023.
- [23] Chunbo Lang, Gong Cheng, Binfei Tu, and Junwei Han. Learning what not to segment: A new perspective on fewshot segmentation. In *Proceedings of the IEEE Conference on Computer Vision and Pattern Recognition*, 2022.
- [24] Boyi Li, Kilian Q Weinberger, Serge Belongie, Vladlen Koltun, and Rene Ranftl. Language-driven semantic segmentation. In *Proceedings of the International Conference on Learning Representations*, 2022.
- [25] Peike Li, Yunchao Wei, and Yi Yang. Consistent structural relation learning for zero-shot segmentation. *Advances in Neural Information Processing Systems*, 2020.
- [26] Feng Liang, Bichen Wu, Xiaoliang Dai, Kunpeng Li, Yinan Zhao, Hang Zhang, Peizhao Zhang, Peter Vajda, and Diana Marculescu. Open-vocabulary semantic segmentation with mask-adapted clip. *Proceedings of the IEEE Conference on Computer Vision and Pattern Recognition*, 2023.
- [27] Tsung-Yi Lin, Michael Maire, Serge Belongie, James Hays, Pietro Perona, Deva Ramanan, Piotr Dollár, and C Lawrence Zitnick. Microsoft coco: Common objects in context. In *Proceedings of the European Conference on Computer Vision*, 2014.
- [28] Jinxiang Liu, Chen Ju, Weidi Xie, and Ya Zhang. Exploiting transformation invariance and equivariance for self-supervised sound localisation. In *Proceedings of ACM International Conference on Multimedia*, 2022.
- [29] Yongfei Liu, Xiangyi Zhang, Songyang Zhang, and Xuming He. Part-aware prototype network for few-shot semantic segmentation. *Proceedings of the European Conference on Computer Vision*, 2020.
- [30] Zhihe Lu, Sen He, Xiatian Zhu, Li Zhang, Yi-Zhe Song, and Tao Xiang. Simpler is better: Few-shot semantic segmentation with classifier weight transformer. *Proceedings of the International Conference on Computer Vision*, 2021.
- [31] Chaofan Ma, Yuhuan Yang, Chen Ju, Fei Zhang, Jinxiang Liu, Yu Wang, Ya Zhang, and Yanfeng Wang. Diffusionseg: Adapting diffusion towards unsupervised object discovery. *arXiv preprint arXiv:2303.09813*, 2023.
- [32] Chaofan Ma, Yuhuan Yang, YanFeng Wang, Ya Zhang, and Weidi Xie. Open-vocabulary semantic segmentation with frozen vision-language models. In *Proceedings of the British Machine Vision Conference*, 2022.
- [33] Juhong Min, Dahyun Kang, and Minsu Cho. Hypercorrelation squeeze for few-shot segmentation. In *Proceedings of the International Conference on Computer Vision*, 2021.
- [34] Shujon Naha, Qingyang Xiao, Prianka Banik, Md Alimoor Reza, and David J Crandall. Pose-guided knowledge transfer for object part segmentation. In *Proceedings of the IEEE/CVF Conference on Computer Vision and Pattern Recognition Workshops*, 2020.
- [35] Shujon Naha, Qingyang Xiao, Prianka Banik, Md Alimoor Reza, and David J. Crandall. Pose-guided knowledge transfer for object part segmentation. In *2020 IEEE/CVF Conference on Computer Vision and Pattern Recognition Workshops (CVPRW)*, 2020.
- [36] Khoi Nguyen and Sinisa Todorovic. Feature weighting and boosting for few-shot segmentation. In *Proceedings of the International Conference on Computer Vision*, 2019.
- [37] Xuecheng Nie, Jiashi Feng, and Shuicheng Yan. Mutual learning to adapt for joint human parsing and pose estimation. In *Proceedings of the European Conference on Computer Vision*, 2018.
- [38] OpenAI. Gpt-4 technical report, 2023.

- [39] Alec Radford, Jong Wook Kim, Chris Hallacy, Aditya Ramesh, Gabriel Goh, Sandhini Agarwal, Girish Sastry, Amanda Askell, Pamela Mishkin, Jack Clark, Gretchen Krueger, and Ilya Sutskever. Learning transferable visual models from natural language supervision. In *Proceedings of the International Conference on Machine Learning*, 2021.
- [40] René Ranftl, Alexey Bochkovskiy, and Vladlen Koltun. Vision transformers for dense prediction. In *Proceedings of the International Conference on Computer Vision*, 2021.
- [41] Olaf Ronneberger, Philipp Fischer, and Thomas Brox. U-net: Convolutional networks for biomedical image segmentation. In *Medical Image Computing and Computer-Assisted Intervention*, 2015.
- [42] Amirreza Shaban, Shray Bansal, Liu Zhen, Irfan Essa, and Byron Boots. One-shot learning for semantic segmentation. In *Proceedings of the British Machine Vision Conference*, 2017.
- [43] Evan Shelhamer, Jonathan Long, and Trevor Darrell. Fully convolutional networks for semantic segmentation. *IEEE Transactions on Pattern Analysis and Machine Intelligence*, 2017.
- [44] Alexey A Shvets, Alexander Rakhlin, Alexandr A Kalinin, and Vladimir I Iglovikov. Automatic instrument segmentation in robot-assisted surgery using deep learning. In *2018 17th IEEE international conference on machine learning and applications (ICMLA)*, 2018.
- [45] Robin Strudel, Ricardo Garcia, Ivan Laptev, and Cordelia Schmid. Segmenter: Transformer for semantic segmentation. In *Proceedings of the International Conference on Computer Vision*, 2021.
- [46] Zhuotao Tian, Xin Lai, Li Jiang, Shu Liu, Michelle Shu, Hengshuang Zhao, and Jiaya Jia. Generalized few-shot semantic segmentation. In *Proceedings of the IEEE Conference on Computer Vision and Pattern Recognition*, 2022.
- [47] Zhuotao Tian, Hengshuang Zhao, Michelle Shu, Zhicheng Yang, Ruiyu Li, and Jiaya Jia. Prior guided feature enrichment network for few-shot segmentation. *IEEE Transactions on Pattern Analysis and Machine Intelligence*, 2020.
- [48] Haochen Wang, Xudong Zhang, Yutao Hu, Yandan Yang, Xianbin Cao, and Xiantong Zhen. Few-shot semantic segmentation with democratic attention networks. *Proceedings of the European Conference on Computer Vision*, 2020.
- [49] Kaixin Wang, Jun Hao Liew, Yingtian Zou, Daquan Zhou, and Jiashi Feng. Panet: Few-shot image semantic segmentation with prototype alignment. In *Proceedings of the International Conference on Computer Vision*, 2019.
- [50] Yongqin Xian, Subhabrata Choudhury, Yang He, Bernt Schiele, and Zeynep Akata. Semantic projection network for zero-and few-label semantic segmentation. In *Proceedings of the IEEE Conference on Computer Vision and Pattern Recognition*, 2019.
- [51] Enze Xie, Wenhai Wang, Zhiding Yu, Anima Anandkumar, Jose M Alvarez, and Ping Luo. Segformer: Simple and efficient design for semantic segmentation with transformers. In *Advances in Neural Information Processing Systems*, 2021.
- [52] Hu Xu, Gargi Ghosh, Po-Yao Huang, Dmytro Okhonko, Armen Aghajanyan, Florian Metze, Luke Zettlemoyer, and Christoph Feichtenhofer. Videoclip: Contrastive pre-training for zero-shot video-text understanding. *arXiv preprint arXiv:2109.14084*, 2021.
- [53] Mengde Xu, Zheng Zhang, Fangyun Wei, Yutong Lin, Yue Cao, Han Hu, and Xiang Bai. A simple baseline for open vocabulary semantic segmentation with pre-trained vision-language model. *Proceedings of the European Conference on Computer Vision*, 2022.
- [54] Lewei Yao, Runhui Huang, Lu Hou, Guansong Lu, Minzhe Niu, Hang Xu, Xiaodan Liang, Zhenguo Li, Xin Jiang, and Chunjing Xu. Filip: Fine-grained interactive language-image pre-training. In *Proceedings of the International Conference on Learning Representations*, 2022.
- [55] Han-Jia Ye, Hexiang Hu, and De-Chuan Zhan. Learning adaptive classifiers synthesis for generalized few-shot learning. *International Journal of Computer Vision*, 2021.
- [56] Lu Yuan, Dongdong Chen, Yi-Ling Chen, Noel Codella, Xiyang Dai, Jianfeng Gao, Houdong Hu, Xuedong Huang, Boxin Li, Chunyuan Li, et al. Florence: A new foundation model for computer vision. *arXiv preprint arXiv:2111.11432*, 2021.
- [57] Xiaohua Zhai, Xiao Wang, Basil Mustafa, Andreas Steiner, Daniel Keysers, Alexander Kolesnikov, and Lucas Bayer. Lit: Zero-shot transfer with locked-image text tuning. In *Proceedings of the IEEE Conference on Computer Vision and Pattern Recognition*, 2022.

- [58] Bingfeng Zhang, Jimin Xiao, and Terry Qin. Self-guided and cross-guided learning for few-shot segmentation. *Proceedings of the IEEE Conference on Computer Vision and Pattern Recognition*, 2021.
- [59] Chi Zhang, Guosheng Lin, Fayao Liu, Rui Yao, and Chunhua Shen. Canet: Class-agnostic segmentation networks with iterative refinement and attentive few-shot learning. *Proceedings of the IEEE Conference on Computer Vision and Pattern Recognition*, 2019.
- [60] Gengwei Zhang, Guoliang Kang, Yi Yang, and Yunchao Wei. Few-shot segmentation via cycle-consistent transformer. *Advances in Neural Information Processing Systems*, 2021.
- [61] Jian-Wei Zhang, Yifan Sun, Yi Yang, and Wei Chen. Feature-proxy transformer for few-shot segmentation. *Advances in Neural Information Processing Systems*, 2022.
- [62] Peisen Zhao, Lingxi Xie, Chen Ju, Ya Zhang, Yanfeng Wang, and Qi Tian. Bottom-up temporal action localization with mutual regularization. In *Proceedings of the European Conference on Computer Vision*, 2020.